JACS
JOURNAL OF THE AMERICAN CHEMICAL SOCIETY

Communication

pubs.acs.org/JACS

Nuclear-Targeted Drug Delivery of TAT Peptide-Conjugated Monodisperse Mesoporous Silica Nanoparticles

Limin Pan, Qianjun He, Jianan Liu, Yu Chen, Ming Ma, Linlin Zhang, and Jianlin Shi*

State Key Laboratory of High Performance Ceramics and Superfine Microstructure, Shanghai Institute of Ceramics, Chinese Academy of Sciences, 1295 Ding-Xi Road, Shanghai 200050, China

Supporting Information

ABSTRACT: Most present nanodrug delivery systems have been developed to target cancer cells but rarely nuclei. However, nuclear-targeted drug delivery is expected to kill cancer cells more directly and efficiently. In this work, TAT peptide has been employed to conjugate onto mesoporous silica nanoparticles (MSNs-TAT) with high payload for nuclear-targeted drug delivery for the first time. Monodispersed MSNs-TAT of varied particle sizes have been synthesized to investigate the effects of particle size and TAT conjugation on the nuclear membrane penetrability of MSNs. MSNs-TAT with a diameter of 50 nm or smaller can efficiently target the nucleus and deliver the active anticancer drug doxorubicin (DOX) into the targeted nucleus, killing these cancer cells with much enhanced efficiencies. This study may provide an effective strategy for the design and development of cell-nuclear-targeted drug delivery.

Targeted intracellular nanodrug delivery systems (nano-DDSs), which are expected to depress the toxic side effects and simultaneously enhance the therapeutic efficiency, have drawn great attention in the past few years. Recently, various biocompatible nanoparticles with different nanostructures and compositions, such as metals, oxides, semiconductors, polymers, and nanomagnets, have been employed as nano-DDSs to target cancer cells.[1−8] However, most of these investigations have concerned the intracellular localization of nanoparticles mainly in the cytoplasm and rarely in the cell nucleus. In fact, the cell nucleus is the final targeting destination because it is the cellular "heart", where the genetic information and the transcription machinery reside and also where numerous therapeutic agents efficiently work. Typically, gene therapy aims at correcting disfunctional and/or missing genes by delivering therapeutic genes into the cell nucleus.[9] In addition, some anticancer agents, such as the typical anticancer drug doxorubicin (DOX), can induce apoptosis of tumor cells mainly by oxidative DNA damage and topoisomerase II inhibition in the nucleus.[10] However, it is quite difficult for free anticancer drugs/DNA to keep active after arriving at the nucleus because of the many biobarriers.[10] Therefore, the development of nuclear-targeted nano-DDSs is expected to provide significantly enhanced anticancer efficiency of presently available drugs and is thus of great importance. Among available nanomaterials for drug delivery, mesoporous silica nanoparticles (MSNs) have been well-demonstrated as excellent carriers for drug delivery because of their unique properties, such as high drug loading capability resulting from their high specific surface area and large pore volume, facile tuning of the particle size over a broad range, easy surface modification/bioconjugation for targeting, and high biochemical and physicochemical stability.[11] However, to the best of our knowledge, there has been no report about the construction of MSN-based nuclear-targeted nano-DDSs, though a few types of bioconjugated MSNs have been constructed to target cell membranes.[12−17]

It is known that the nuclear envelope consists of a nuclear membrane embedded with plenty of nuclear pore complexes (NPCs) with a diameter of 20−70 nm, which is dependent on the cell type and cell cycle.[18] NPCs are the unique available/mediatable passages for all exchange between the nucleoplasm and cytoplasm that also provide the pathways for nanoparticle entrance.[19] The intranuclear transport of large heterogeneous nanoparticles can be triggered with the facilitation of a nuclear localization signal (NLS).[20] Several kinds of functional nanoparticles [e.g., silver nanoparticles, quantum dots (QDs), magnetic nanoparticles, etc.] have been reported to be able to target nuclei through conjugation of NLSs to the surface of the nanoparticles.[21−24] In the case of gold nanoparticles, several cancer cell nucleus-targeted delivery strategies have been developed by decorating the surfaces of nanoparticles with different NLS peptides, such as SV40 T antigen, HIV-1 TAT peptide, and adenoviral.[7,25,26] Among these NLS peptides, TAT peptide has been shown to be an efficient molecule for translocating nanoparticles into cell nuclei via the binding import receptors importin α and β (karyopherin) and subsequently targeting the NPCs of cancer cells and entering their nuclei.[27−29] Herein we report a novel nuclear-targeted nano-DDS based on TAT peptide-conjugated MSNs (MSNs-TAT) that facilitates nuclear internalization and the release of the encapsulated drugs within the nucleoplasm. Figure 1A illustrates the procedures for the preparation of MSNs and the subsequent surface modification with TAT peptide. Therefore by such a nuclear-targeted mechanism, the present DOX-loaded MSNs-TAT (DOX@MSNs-TAT) are expected to target nuclei of cancer cells and then deliver/release drugs directly into nuclei, as illustrated in Figure 1B.

As mentioned above, a small enough particle size is an important prerequisite to ensure that the nanoparticles can step across NPCs. Therefore, MSNs of four different particle sizes

Received: November 24, 2011
Published: March 15, 2012

   dx.doi.org/10.1021/ja211035w | J. Am. Chem. Soc. 2012, 134, 5722−5725

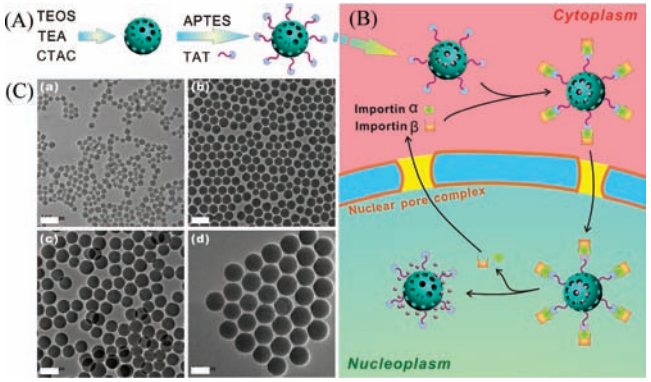

Figure 1. (A) Schematic diagram of the procedures for preparating amine group- and TAT-C6-FITC peptide-conjugated MSNs. (B) Schematic illustration of transport of DOX@MSNs-TAT across the nuclear membrane. (C) TEM images of MSNs with sizes of (a) 25, (b) 50, (c) 67, and (d) 105 nm. Scale bars: 100 nm.

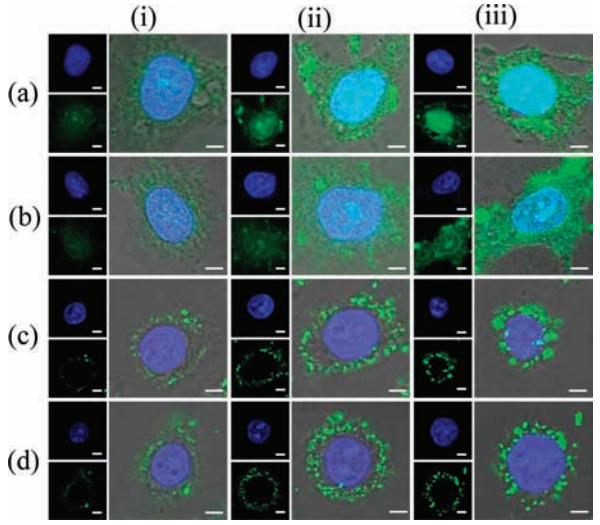

Figure 2. CLSM images of MSNs-TAT with diameters of (a) 25, (b) 50, (c) 67, and (d) 105 nm after incubation with Hela cells for (i) 4, (ii) 8, and (iii) 24 h. Scale bars: 5 μm.

were synthesized in order to investigate the effect of particle size on the nuclear internalization by cancer cells. Typically, highly dispersed MSNs with uniform and tunable particle size were prepared following the protocol proposed by Bein and co-workers with a certain modification.[30] Figure 1 and Figure S1 in the Supporting Information show that the four MSN samples had uniform particle sizes (25, 50, 67, and 105 nm) and that both the MSNs and MSNs-TAT could be thoroughly dispersed in PBS. The dynamic light scanning (DLS) diameters (Tables S1 and S2 and Figure S2) were larger than the transmission electron microscopy (TEM) diameters to some varied extents due to the presence of the hydrated layers around the particle surfaces. Moreover, the wormlike mesoporous structures with pore sizes of 2−3 nm could be observed from the TEM images (Figure 1C), which could also be confirmed by the absence of corresponding small-angle X-ray diffraction peak(s) (Figure S3). Nitrogen adsorption−desorption isotherm measurements indicated that these MSNs samples possessed relatively high specific surface areas of 390−561 m^2/g and well-defined pore sizes of ∼2.7 nm (Figure S4 and Table S1), in accordance with the TEM results. In addition, FT-IR measurements showed that the surfactant CTAC was completely removed by the extraction procedure according to the absence of the characteristic C−H peak in the 3000−2800 cm^{-1} wavelength range for the surfactant-extracted MSNs (Figure S5). The complete extraction of the template ensured the high biocompatibility of the carriers and the loading of anticancer drugs. Furthermore, the conjugation of TAT peptide on the outside surface of the MSNs by an esterification reaction was confirmed by UV−vis absorbance spectrometry, as clearly indicated by the disappearance of the characteristic absorption bands of fluorescein isothiocyanate (FITC) at the N-termini of the TAT peptides and also the color change of the MSNs-TAT solution after centrifugation (Figure S6 inset).

To investigate cellular uptake of MSNs and MSNs-TAT of varied particle sizes, they were coincubated with Hela cells at the same concentration of 0.1 mg mL^{-1} and observed using confocal laser scanning microscopy (CLSM). The cellular uptake and subsequent localization of differently sized MSNs-TAT for 4, 8, and 24 h incubations are shown in Figure 2. It can be first seen from the figure that there were very few nanoparticles in the nuclei after 4 h, regardless of the particle size. Importantly, MSNs-TAT of 25 and 50 nm in diameter can be clearly seen in both the cytoplasm and the nuclei of Hela cells after incubation for 8 and 24 h, as demonstrated by the green fluorescence from FITC lighting up the nuclei. Comparatively, both 67 and 105 nm-sized MSNs-TAT are mainly located in the cytoplasm and the perinuclear region after the same durations of incubation. It is concluded that the MSNs-TAT of or smaller than 50 nm in diameter can penetrate into nuclei beginning from 4 h. The Bio-TEM images after incubation with these particles for 24 h (Figure S7) support our claims very well. We can clearly see MSNs-TAT (25 and 50 nm) inside the nuclei and 67 and 105 nm ones outside the nuclei in this figure. The existence of silicon in the nuclei from energy-dispersive X-ray (EDX) analysis further proved the nuclear localization of 25 and 50 nm MSNs-TAT. The present results are comparable to the conclusion drawn by Panté and Kann[31] that gold nanoparticles with a diameter close to 39 nm could be translocated into the cell nucleus. Besides, TAT peptide was able to import 90 nm beads into the nuclei of digitonin-permeabilized cells.[32] The nuclear localization of 25 and 50 nm MSNs-TAT provides an excellent platform for intranuclear drug delivery. In addition, lower-magnification confocal images (Figure S8) further confirmed the effective intranuclear localization of the 25 and 50 nm MSNs-TAT.

To evidence the decisive role of the surface-conjugated TAT peptide in the nuclear localization, FITC-labeled MSNs with the same diameters were also incubated with Hela cells under the same conditions, and the uptake process was monitored in the same way; the results are shown in Figure S9. To trace the nanoparticles, FITC was grafted on the inner pore surface of MSNs by a cocondensation route.[33] All of the MSNs were distributed in the cell cytoplasm randomly, and no particles were found inside the nuclei in 24 h time frame. On the basis of the above findings of the nuclear penetration threshold of Hela cells, the exclusion of 67 and 105 nm-sized MSNs out of nuclei was expected. However, the MSNs with diameters of 25 and 50 nm that met the size requirement of intranuclear localization were also blocked out of the nuclei, indicating the vital role of surface-conjugated TAT peptide in the nanoparticle intranuclear translocation. There was no NLS on the MSNs to interact with the receptors, importin α and β, leading to the failure in the recognition of the cargos by NPCs. It is concluded that TAT peptide is an indispensable medium for interacting

dx.doi.org/10.1021/ja211035w | J. Am. Chem. Soc. 2012, 134, 5722−5725

with NPCs and realizing nuclear targeting and penetration. As expected, the unconjugated MSNs were not found in the nuclei after incubation with Hela cells for shorter time periods of 4 and 8 h.

As a negative control, the cellular uptake of MSNs in the presence of free TAT peptide was also carried out. As shown in Figure S10, the distribution of MSNs in the cytoplasm indicated that the free TAT peptide had no detectable positive effects on the nuclear translocation of MSNs. The nuclear uptakes of MSNs and MSNs-TAT were further confirmed by nuclear silicon quantification via extraction of nuclei from the cells. The results in Figure S11 show that the nuclear uptake of MSNs was approximately equivalent to that of MSNs in the presence of free TAT peptide, demonstrating that free TAT peptide does not facilitate the nuclear location of MSNs. Moreover, the nuclear uptakes of MSNs-TAT were 21.5- and 49-fold higher than those of MSNs at diameters of 25 and 50 nm, respectively. Reasonably, there was no distinct difference in the nuclear uptakes of MSNs and MSNs-TAT with diameters of 67 and 105 nm.

As a direct test of intranuclear drug delivery by MSNs-TAT, we loaded them with the anticancer drug DOX. The drug loading capacities are shown in Table S2, and one can see that TAT modification had a negligible influence on the capacity. It is commonly accepted that DOX, a typical and widely used anticancer drug, shows a pharmacodynamic effect in nuclei by damaging the DNA structure.[34,35] To investigate the cellular internalization and the intracellular and intranuclear releases of DOX, DOX@MSNs (25 nm) and DOX@MSNs-TAT (25 nm) were incubated with Hela cells for 4 h at 37 °C. Red fluorescence imaging was performed to visualize the released DOX (Figure 3). For free DOX, the red fluorescence was

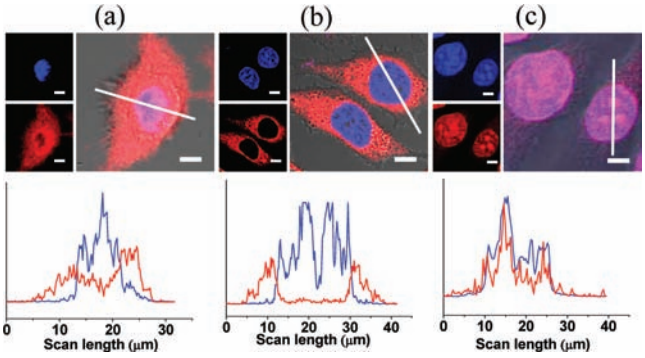

Figure 3. (top) CLSM images and (bottom) line-scan profiles of fluorescence intensity for Hela cells incubated for 4 h with (a) free DOX, (b) DOX@MSNs (25 nm), and (c) DOX@MSNs-TAT (25 nm). The red fluorescence is from DOX, and the blue fluorescence is from 4,6-diamidino-2-phenylindole (DAPI) used to stain the nuclei. The concentration of DOX was 5 μg mL^{-1}. Scale bars: 5 μm.

spread all over the cells, mostly in the cytoplasm with a small amount in the nuclei, due to a concentration gradient diffusion mechanism of free DOX. In the case of DOX@MSNs-TAT, the red fluorescence is highly accumulated in nuclei, which is exactly opposite to the case of DOX@MSNs, indicating the nuclear localization of DOX@MSNs-TAT. There was very slight red fluorescence in the nuclei in the case of DOX@MSNs, demonstrating that DOX cannot be directly delivered into nuclei by unconjugated DOX@MSNs and confirming the DOX release in a slow and sustained way in the cytoplasm. It can also be known that the red fluorescence in Figure 3c is from the DOX@MSNs-TAT conjugation rather than from free DOX that had been released from the DOX@MSNs-TAT in the cytoplasm and then diffused into nuclei. The above observations are more qualitatively confirmed by the line scanning profiles of fluorescent intensity of the selected Hela cells, as also given in Figure 3.

To find any possible enhancement of anticancer efficiency of the DOX@MSNs-TAT nano-DDSs, the cytotoxicity of the carriers was first measured by in vitro MTT assay (Figure S12). The cell viability of Hela cells remained above 80% when they were treated with the four differently sized MSNs and MSNs-TAT up to a concentration of 1 mg mL^{-1} for 24 h. This is consistent with the previous finding that silica is not intrinsically toxic, though more in-depth investigations are needed to rule out completely possible hazards related to the tiny dimensions of the nanoparticles.[36] Next, the cytotoxic effects of DOX@MSNs-TAT against Hela cells were tested. As shown in Figure 4, both 25 and 50 nm-sized DOX@MSNs-

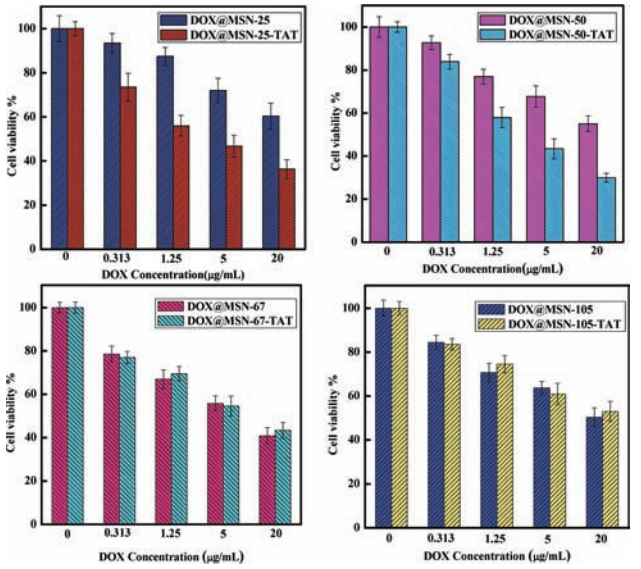

Figure 4. Hela cell viabilities after 24 h of incubation with DOX-loaded MSNs and MSNs-TAT nanoparticles (25, 50, 67, and 105 nm) at different DOX concentrations.

TAT exhibited significantly greater cytotoxicity than DOX-loaded MSNs after coincubation for 24 h at DOX concentrations not higher than 20 μg/mL. However, the DOX@MSNs-TAT with diameters of 67 and 105 nm exhibited no greater cytotoxicity than corresponding DOX-loaded MSNs without TAT modification. This is in accordance with the significant intranuclear DOX delivery by only the 25 and 50 nm-sized DOX@MSNs-TAT. As a further verification of this conclusion, the size-dependent cellular uptakes of the four sizes of MSNs and MSNs-TAT are shown in Figure S13. We found that the particle-size-dependent cellular uptakes of MSNs and MSNs-TAT by Hela cells occurred in the particle size order of 50 > 67 > 25 > 105 nm, similar to the previous report by Mou and co-workers.[37] On the other hand, because of the presence of TAT, the cellular uptake of MSNs-TAT was higher than that of the corresponding MSNs of the same diameter. The higher cellular uptake but lower anticancer activity of 67 nm MSNs-TAT relative to the 25 nm ones indicates that the nuclear penetration of 25 nm DOX@MSNs-TAT makes a great contribution to the enhanced therapeutic efficacy. The

dx.doi.org/10.1021/ja211035w | J. Am. Chem. Soc. 2012, 134, 5722–5725

conjugated TAT peptide promoted the intranuclear distribution of DOX@MSNs-TAT, after which the DOX molecules remaining in the MSNs-TAT were released within the nuclei, and the anticancer activity was enhanced along with the increase in the intranuclear DOX concentration. Especially for 50 nm DOX@MSNs-TAT, only about 30% of the cells survived after 24 h of incubation. The clear contrasts in the viabilities of cells treated with free DOX, DOX@MSNs, and DOX@MSNs-TAT obtained from the in vitro MTT assay for different incubation time durations (Figure S14) further evidence the positive effects of cellular uptake of the nano-DDSs and especially the intranuclear localizations of the MSNs-TAT conjugates on the cytotoxicity. The sustained DOX release from the nano-DDS (Figure S15) should be responsible for the lower cytotoxicity of the nano-DDS than free drug (in first 1 h) and the gradually enhanced cytotoxicity at prolonged incubation (Figure S14). The DOX@MSNs-TAT entrapped in nuclei can release DOX intranuclearly and sustainably, leading to much lowered cell viability in 24 h, which demonstrates the high effectiveness of the nuclear-targeted drug delivery.

In summary, we have constructed 25−105 nm-sized peptide−MSN conjugates for targeting cell nuclei. The presence of TAT peptide facilitates the active nuclear entry of MSNs through the nuclear pore complexes, while the size of the MSNs-TAT is a critical factor in the translocation. A nano-DDS of 25−50 nm-sized MSNs conjugated with TAT peptide in this study has been proved to be suitable for transport across the nuclear membrane. The nuclear-targeted and intranuclear DOX delivery by the above-mentioned nano-DDS demonstrated a significant enhancement in the anticancer activity of the drug. We anticipate that the aforementioned MSNs-TAT conjugate may be a promising starting point for the fabrication of multifunctional nanomaterials for nuclear-targeted drug delivery for cancer therapy.

■ ASSOCIATED CONTENT

Supporting Information

Experimental details and characterization data. This material is available free of charge via the Internet at http://pubs.acs.org.

■ AUTHOR INFORMATION

Corresponding Author

jlshi@sunm.shcnc.ac.cn

Notes

The authors declare no competing financial interest.

■ ACKNOWLEDGMENTS

This work was financially supported by the National Natural Science Foundation of China (Grants 51102259, 50823007, 51132009, and 50972154), the Science and Technology Commission of Shanghai (Grants 10430712800, 11 nm0505000, and 11 nm0506500), and the Science Foundation for Youth Scholar of State Key Laboratory of High Performance Ceramics and Superfine Microstructures (Grant SKL201001).

■ REFERENCES

(1) West, J. L.; Halas, N. J. *Curr. Opin. Biotechnol.* **2000**, *11*, 215.
(2) Högemann, D.; Ntziachristos, V.; Josephson, L.; Weissleder, R. *Bioconjugate Chem.* **2002**, *13*, 116.
(3) Bruchez, M.; Moronne, M.; Gin, P.; Weiss, S.; Alivisatos, A. P. *Science* **1998**, *281*, 2013.
(4) Liu, J.; Zhang, Q.; Remsen, E. E.; Wooley, K. L. *Biomacromolecules* **2001**, *2*, 362.
(5) Marinakos, S. M.; Anderson, M. F.; Ryan, J. A.; Martin, L. D.; Feldheim, D. L. *J. Phys. Chem. B* **2001**, *105*, 8872.
(6) Feldherr, C. M.; Lanford, R. E.; Akin, D. *Proc. Natl. Acad. Sci. U.S.A.* **1992**, *89*, 11002.
(7) Tkachenko, A. G.; Xie, H.; Coleman, D.; Glomm, W.; Ryan, J.; Anderson, M. F.; Franzen, S.; Feldheim, D. L. *J. Am. Chem. Soc.* **2003**, *125*, 4700.
(8) Kim, J.; Lee, J. E.; Lee, S. H.; Yu, J. H.; Lee, J. H.; Park, T. G.; Hyeon, T. *Adv. Mater.* **2008**, *20*, 478.
(9) van der Aa, M. A. E. M.; Mastrobattista, E.; Oosting, R. S.; Hennink, W. E.; Koning, G. A.; Crommelin, D. J. A. *Pharm. Res.* **2006**, *23*, 447.
(10) Mizutani, H.; Tada-Oikawa, S.; Hiraku, Y.; Kojima, M.; Kawanishi, S. *Life Sci.* **2005**, *76*, 1439.
(11) Slowing, I. I.; Vivero-Escoto, J. L.; Wu, C. W.; Lin, V. S. Y. *Adv. Drug Delivery Rev.* **2008**, *60*, 1278.
(12) Vivero-Escoto, J. L.; Slowing, I. I.; Trewyn, B. G.; Lin, V. S. Y. *Small* **2010**, *6*, 1952.
(13) Liong, M.; Lu, J.; Kovochich, M.; Xia, T.; Ruehm, S. G.; Nel, A. E.; Tamanoi, F.; Zink, J. I. *ACS Nano* **2008**, *2*, 889.
(14) Rosenholm, J. M.; Meinander, A.; Peuhu, E.; Niemi, R.; Eriksson, J. E.; Sahlgren, C.; Linden, M. *ACS Nano* **2009**, *3*, 197.
(15) Rosenholm, J.; Sahlgren, C.; Linden, M. *J. Mater. Chem.* **2010**, *20*, 2707.
(16) Rosenholm, J. M.; Peuhu, E.; Eriksson, J. E.; Sahlgren, C.; Linden, M. *Nano Lett.* **2009**, *9*, 3308.
(17) Rosenholm, J. M.; Peuhu, E.; Bate-Eya, L. T.; Eriksson, J. E.; Sahlgren, C.; Linden, M. *Small* **2010**, *6*, 1234.
(18) Kubitscheck, U.; Grnwald, D.; Hoekstra, A.; Rohleder, D.; Kues, T.; Siebrasse, J. P.; Peters, R. J. *Cell Biol.* **2005**, *168*, 233.
(19) Meinema, A. C.; Laba, J. K.; Hapsari, R. A.; Otten, R.; Mulder, F. A. A.; Kralt, A.; van den Bogaart, G.; Lusk, C. P.; Poolman, B.; Veenhoff, L. M. *Science* **2011**, *333*, 90.
(20) Kang, B.; Megan, A. M.; Mostafa, A. E. *J. Am. Chem. Soc.* **2010**, *132*, 1517.
(21) Austin, L. A.; Kang, B.; Yen, C. W.; El-Sayed, M. A. *Bioconjugate Chem.* **2011**, *22*, 2324.
(22) Austin, L. A.; Kang, B.; Yen, C. W.; El-Sayed, M. A. *J. Am. Chem. Soc.* **2011**, *133*, 17594.
(23) Chen, F.; Gerion, D. *Nano Lett.* **2004**, *4*, 1827.
(24) Xu, C.; Xie, J.; Kohler, N.; Walsh, E. G.; Chin, Y. E.; Sun, S. *Chem.—Asian. J.* **2008**, *3*, 548.
(25) Lin, S.; Chen, N.; Sun, S.; Chang, J.; Wang, Y.; Yang, C.; Lo, L. *J. Am. Chem. Soc.* **2010**, *132*, 8309.
(26) Fuente, J.; Berry, C. C. *Bioconjugate Chem.* **2005**, *16*, 1176.
(27) Nakielny, S.; Dreyfuss, G. *Cell* **1999**, *99*, 677.
(28) Patel, S. S.; Belmont, B. J.; Sante, J. M.; Rexach, M. F. *Cell* **2007**, *129*, 83.
(29) Alber, F.; Dokudovskaya, S.; Veenhoff, L. M.; Zhang, W.; Kipper, J.; Devos, D.; Suprapto, A.; Karni-Schmidt, O.; Williams, R.; Chait, B. T. *Nature* **2007**, *450*, 695.
(30) Kobler, J.; Möller, K.; Bein, T. *ACS Nano* **2008**, *2*, 791.
(31) Panté, N.; Kann, M. *Mol. Biol. Cell* **2002**, *13*, 425.
(32) Nitin, N.; Conte, L.; Rhee, W. J.; Bao, G. *Ann. Biomed. Eng.* **2009**, *37*, 2018.
(33) He, Q.; Shi, J.; Cui, X.; Zhao, J.; Chen, Y.; Zhou, J. *J. Mater. Chem.* **2009**, *19*, 3395.
(34) dos Santos, R. A.; Jordão, A. A. Jr.; Vannucchi, H.; Takahashi, C. S. *Nutr. Res.* **2007**, *27*, 343.
(35) Yoshida, M.; Shiojima, I.; Ikeda, H.; Komuro, I. *J. Mol. Cell. Cardiol.* **2009**, *47*, 698.
(36) He, Q.; Shi, J.; Zhu, M.; Chen, Y.; Chen, F. *Microporous Mesoporous Mater.* **2010**, *131*, 314.
(37) Lu, F.; Wu, S.; Hung, Y.; Mou, C. *Small* **2009**, *5*, 1408.